XVI International Conference on Computational Plasticity. Fundamentals and Applications
COMPLAS 2021
E. Oñate, D. Peric, M. Chiumenti and Eduardo de Souza Neto (Eds)

EVALUATION OF THERMAL FATIGUE LIFE OF SOLDER JOINTS IN ELECTRONIC DEVICES BASED ON STRESS AND STRAIN SINGULARITY PARAMETERS

JIHONG LIU*

* Technology and Innovation Center (TIC)
Daikin Industries, Ltd.
1-1 Nishi-Hitotsuya, Settsu, Osaka 566-8585, Japan
jihong.liu@daikin.co.jp, www.daikin.com

Key words: Solder Joints, Fatigue Life, Singularity Parameters, Thermal Cycle Test, FEM.

Abstract. It is known that thermal fatigue easily occurs in solder joints of electronic devices. In this study, we proposed a new method to evaluate the thermal fatigue life of the solder joints with the singularity parameters of stress and strain fields near the solder joint edges. Firstly, we constructed creep constitutive equations of the solder materials and confirmed their validity. Next, using zooming analysis based on the finite element method (FEM), we calculated the stress and strain singularity parameters near the solder joint edges for power modules under thermal cycle test conditions. Finally, we obtained evaluation equations of thermal fatigue life for the solder joints by connecting the singularity parameters and the fatigue test results with fatigue laws. It was clarified that the evaluation equations using the singularity parameters are valid and useful for predicting the thermal fatigue life of the solider joints in electronic devices.

1 INTRODUCTION

It is generally known that cracks are likely to occur in the vicinity of solder joints due to repeated temperature changes over a long time, which greatly affect the thermal fatigue life of electronic devices. Currently, the thermal fatigue life of solder joints in electronic devices is evaluated mainly by test methods such as thermal cycle test and power cycle test, but in order to improve the efficiency and completeness of development, it is strongly desired to evaluate the thermal fatigue life of solder joints using analytical methods.

Until now, several studies on the analytical methods of evaluating the thermal fatigue life of solder joints in electronic devices have been conducted [1-4]. In these studies, in order to avoid the singularity of stress and strain fields near the solder joint edges due to dissimilar material bonding, the thermal fatigue life of the solder joints are evaluated using the maximum stress or strain amplitude of a representative point near the solder joint edges. These methods are useful and practical when the solder joints have similar structures and the same calculation accuracy is ensured for stress or strain. However, it is not suitable for generalization because the selection of the representative point involves arbitrariness and trial and error.

Since different materials are combined, the stress and strain fields near the solder joints have singularity. In generally, the behaviours of the singular stress and strain fields can be completely described by the singularity orders and the singularity strength coefficients. Therefore, in this

study, we tried to evaluate the thermal fatigue life of the solder joints using the stress and strain singularity parameters near the solder joint edges. Specifically, firstly, the material properties of the solders were acquired using the material tests and their creep constitutive equations were constructed. Next, the stress and strain singularity parameters in the vicinity of the solder joints for power modules were calculated under the thermal cycle test conditions using FEM analyses. Finally, the stress and strain singularity parameters and the fatigue test results were associated with each other by fatigue laws, and the evaluation equations for predicting the thermal fatigue life of the solder joints were constructed and their accuracy were confirmed reasonably well.

2 MATERIAL PROPERTIES OF SOLDERS

In evaluating the thermal fatigue life of solder joints, it is important to accurately calculate the stress and strain fields near the solder joints that are generated by the load due to temperature changes. Since the solder materials have low melting points and exhibit creep behaviors even at normal temperatures, it is necessary to understand their material properties, especially the temperature dependence of elastic modulus and yield (proof) stress, and the creep constitutive equations. In this section, the material properties of lead solder (Pb-5Sn) and lead-free solder (Sn96.5Ag3.0Cu0.4) are clarified based on the material test results.

2.1 Elastic modulus and yield stress of solders

In the material tests, in order to avoid the influence of load-bearing part of test pieces, the strains are measured using strain gauges attached to both sides of the test piece centers instead of calculating them from the nominal displacements between the gauge points of the test pieces. The static tensile tests for determining the elastic modulus and yield stress of the solders are performed by displacement-controlled loading method, and the effect of differences in loading speed on the test results is also examined.

The changes in the elastic modulus and yield stress of the solders due to the differences in temperature and their approximate expressions are shown in Fig. 1 and 2, respectively. From these figures, it is clarified that the elastic modulus and yield stress of the solders decrease with increasing temperature and have a remarkable temperature dependence. In addition, it can be seen that the elastic modulus and yield stress of lead solder are not affected by the loading speed, whereas, the elastic modulus of lead-free solder is not affected by the loading speed, but its yield stress is affected by the loading speed. It is considered that this is because lead-free solder has a high yield stress, and the tensile test results under high-temperature and high-stress conditions are easily affected by creep deformation. In order to avoid the influence of creep deformation, it is desirable to perform the material tests at a high loading speed (6.0mm/min).

2.2 Creep constitutive equations of solders

The creep tests of the solders are performed by force-controlled loading method. In this section, the creep constitutive equations of the solders are constructed using the creep strain rates and the corresponding stresses, where, the creep strain rates are obtained from the steady-state regions of the creep curves under different stress states and temperature conditions. The creep constitutive equations of the solders can be expressed by a linear viscous function in a low stress state and a hyperbolic function in a high stress state [5].

Based on the creep test results, the creep constitutive equation of lead solder is described in

Eq. (1), where, the temperature range T is from 233.0K to 393.0K, and σ_V is the linear creep limit stress of lead solder, it does not depend on temperature T at low temperatures but becomes a function of temperature T above room temperature. The relationship between the stress of lead solder and the creep strain rate is shown in Fig. 3. It can be read that the creep constitutive equation described in Eq. (1) can accurately express the test results of lead solder.

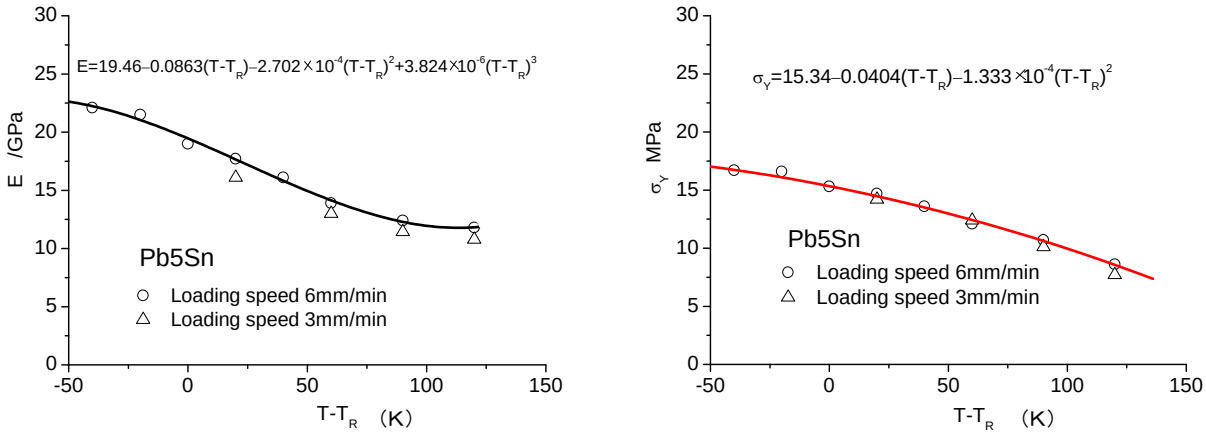

Figure 1: Changes in elastic modulus and yield stress of lead solder due to differences in temperature (T is absolute temperature, T_R is 273.0K)

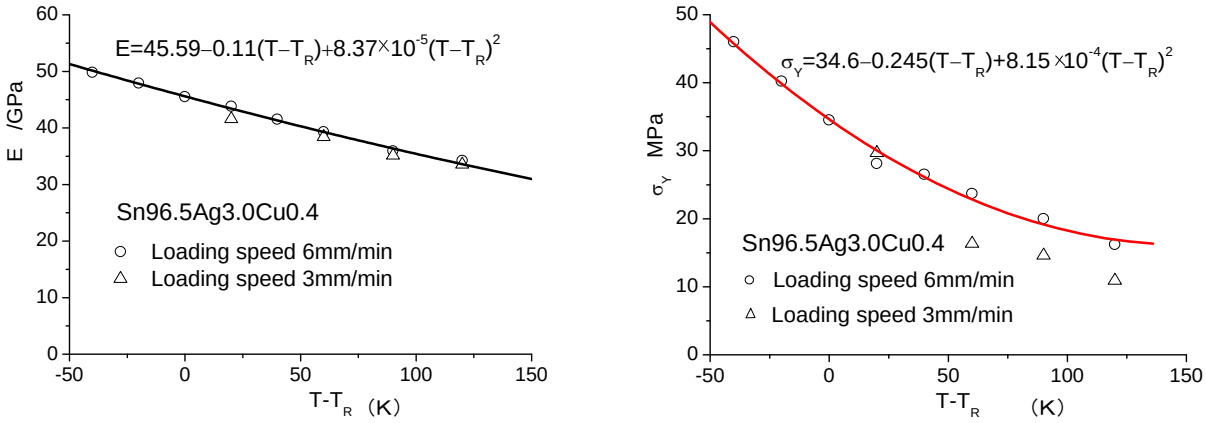

Figure 2: Changes in elastic modulus and yield stress of lead-free solder due to differences in temperature (T is absolute temperature, T_R is 273.0K)

$$
\begin{cases}
T < 273.0K, \sigma_V = 9.5(MPa) & \\
\quad \dfrac{d\epsilon}{dt} = 1.44 \times 10^{-6}[sinh(0.18\sigma)]^{2.35} e^{-\frac{1936.0}{T}} & for\ \sigma \geq \sigma_V \\
\quad \dfrac{d\epsilon}{dt} = (-3.87 \times 10^{-9} + 1.83 \times 10^{-11} T)\sigma & for\ \sigma \leq \sigma_V \\
T > 273.0K, \sigma_V = 14.58 - 0.021T(MPa) & \\
\quad \dfrac{d\epsilon}{dt} = 3.16[sinh(0.18\sigma)]^{4.20} e^{-\frac{6535.0}{T}} & for\ \sigma \geq \sigma_V \\
\quad \dfrac{d\epsilon}{dt} = \left(6.044 \times 10^{-9} - 1.94 \times 10^{-11} T + 0.185 e^{-\frac{5459.0}{T}}\right)\sigma & for\ \sigma \leq \sigma_V
\end{cases}
\tag{1}
$$

The creep constitutive equation of lead-free solder constructed using the creep test results is described in Eq. (2), where, the linear creep limit stress σ_V of lead-free solder is a function of temperature T. The relationship between the stress of lead-free solder and the creep strain rate is shown in Fig. 4. It can be read that the creep constitutive equation of Eq. (2) can accurately express the test results of lead-free solder, except that there are some inappropriate points in the test results at 20.0°C (293.0K) marked with ×. The stresses at these points are low, and the creep strain rates are also low, so it is presumed that a large test error appeared.

3 SINGULAR STRESS AND STRAIN FIELDS AT SOLDER JOINTS

In this section, the stress and strain singularity parameters near the interface edges of the solder joints are obtained using FEM analyses based on the above solder constitutive equations for power modules under thermal cycle test conditions. A schematic diagram of the thermal cycle test conditions is shown in Fig. 5. The power modules are put into an environmental test furnace, and the thermal cycles are repeated from -40.0°C to 80.0°C to -40.0°C. After reaching the specified number of thermal cycles, the rates of increase in electrical resistance at chip ends are measured to determine the number of fatigue life cycles.

In order to calculate the singularity parameters of stress and strain with high accuracy, the stress and strain fields near the interface edges of the solder joints are determined using zooming analysis based on FEM as shown in Fig.6. The detailed analysis procedures are as follows. In this study, the material properties described in Table 1 and Ansys [6] are used for the analyses.

$$
\begin{cases}
T < 283.0K, \sigma_V = 2.55 + 571.3e^{-0.01267/T}(MPa) & \\
\quad \dfrac{d\epsilon}{dt} = 309.03[sinh(0.145\sigma)]^{3.25} e^{-\frac{8765.0}{T}} & for\ \sigma \geq \sigma_V \\
\quad \dfrac{d\varepsilon}{dt} = 2.04 \times 10^{-10}\sigma & for\ \sigma \leq \sigma_V \\
T > 283.0K, \sigma_V = 2.55 + 571.3e^{-0.01267/T}(MPa) & \\
\quad \dfrac{d\epsilon}{dt} = 2.08 \times 10^{-6}[sinh(0.145\sigma)]^{5.85} e^{-\frac{12993.0}{T}} & for\ \sigma \geq \sigma_V \\
\quad \dfrac{d\varepsilon}{dt} = \left(2.04 \times 10^{-10} + 1.10 \times 10^{-3} e^{-\frac{5263.0}{T}}\right)\sigma & for\ \sigma \leq \sigma_V
\end{cases}
\tag{2}
$$

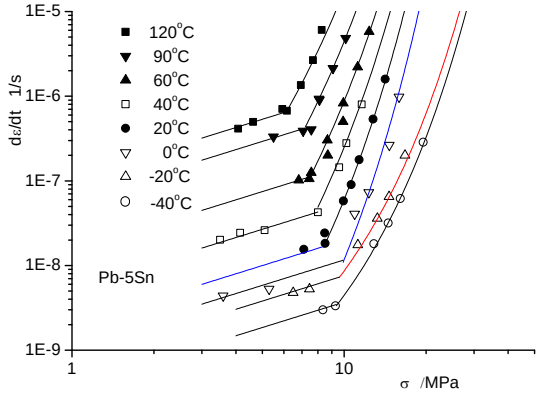

Figure 3: Creep strain rate and stress of lead solder

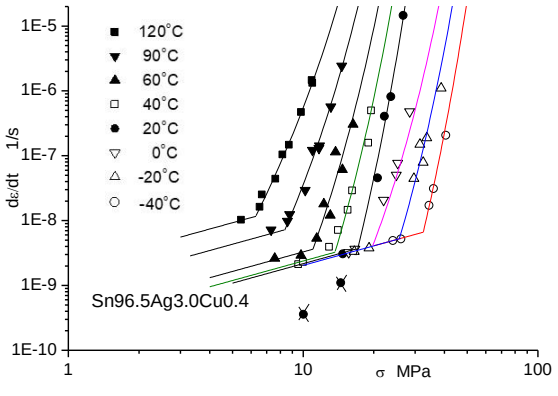

Figure 4: Creep strain rate and stress of lead-free solder

1) Perform unsteady heat conduction analysis using the full model shown in Fig.7 to obtain the temperature distribution in the power module. In the analysis, natural convection conditions are specified between the surface of the power module and the surrounding environment in the test furnace.
2) Conduct nonlinear thermal stress analysis with the full model to determine the thermal stress and strain distribution and deformation of the power module. In the analysis, constraints are applied as boundary conditions so that rigid body displacements do not occur in the power module, and the temperature distribution obtained by the unsteady heat conduction analysis in 1) is used as the load conditions. The temperature dependence of elastic modulus and yield stress, as well as creep characteristics of the solders shown in the previous section are considered in the analysis.
3) The detailed stress and strain distribution near the interface edges of the solder joints of each chip are calculated using the zooming partial model shown in Fig. 8. In this analysis, the displacement distribution obtained using the full model in 2) is linearly interpolated and specified as the boundary conditions, and the temperature distribution obtained using the full model in 1) is linearly interpolated and specified as the load conditions for the zooming partial model, respectively.
4) The chip has a multi-layer structure with different mechanical and thermal properties as shown in Fig. 8. It is clear that there are singular stress and strain fields at the interface edge between the chip 1 and the lead solder 2 (hereinafter referred to as E12), and at the interface edge between the lead-free solder 4 and the circuit pattern 5 (hereinafter referred to as E45).

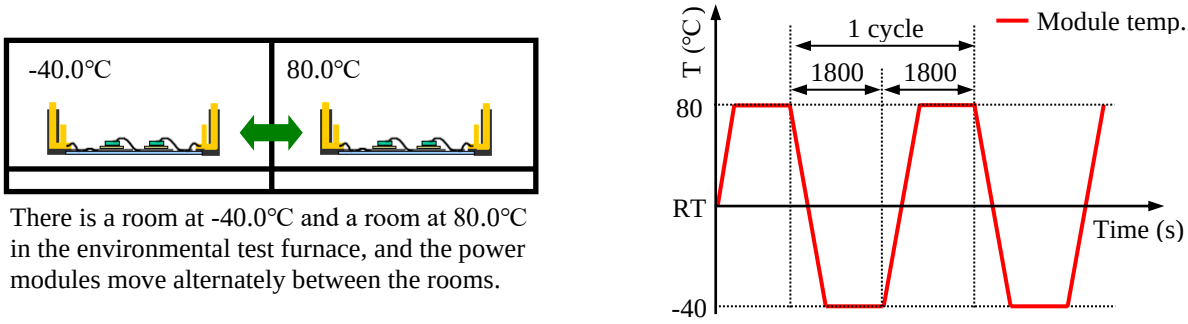

Figure 5: Schematic of thermal cycle test conditions (RT: Room Temperature)

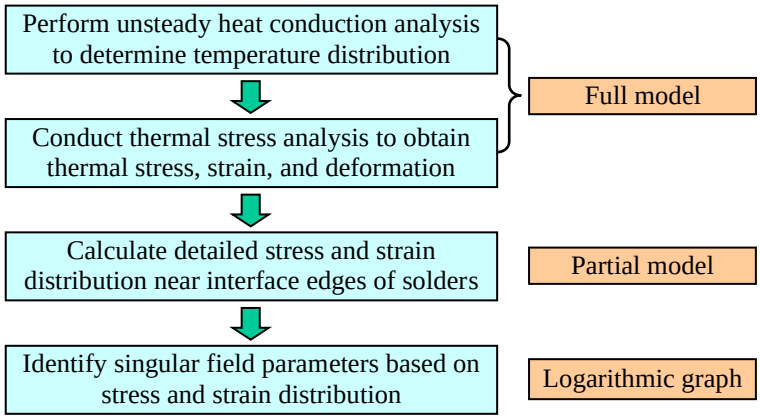

Figure 6: Calculation flow of stress and strain singular field parameters at the interface edges of the solder joints

In general, the singular stress and strain fields near the solder joint interface edges can be expressed in Eq. (3), where, t represents time, and $i = e, 1, 2$ represent equivalent stress, normal stress and shear stress, respectively. As for strain, only equivalent strain is considered. The singularity orders $\delta(t)$, $\varsigma(t)$ and the singularity strength coefficients $K_i(t)$, $K_\varepsilon(t)$ are the functions of time t, respectively, and can be obtained by numerical analyses. Specifically, the slopes of the linear diagrams obtained when the stress or strain distribution near the interface edge of the solder joint are displayed in logarithmic form are the stress or strain singularity orders. The singularity strength coefficients of the corresponding stress or strain are obtained from the constants of the corresponding diagram functions or by extrapolation method. Since the amplitude of the singularity parameters of the maximum stress or strain are important in the evaluation of fatigue life, we focus on the singularity parameters under the maximum and minimum stress or strain states under the thermal cycle test conditions.

$$\sigma_i = \frac{K_i(t)}{r^{\delta(t)}}, \quad \varepsilon_e = \frac{K_\varepsilon(t)}{r^{\varsigma(t)}}, \quad i = e, 1, 2 \tag{3}$$

As an example, the maximum stress and strain distribution near E12 is shown in Fig. 9. It is clarified that the stress and strain distribution in logarithmic form is a straight line, respectively, which shows good linearity near the interface edge of the solder joint. From these straight lines, the singularity parameters of the stress and strain fields can be identified with high accuracy.

From SEM (Scanning Electron Microscope) observations of a power module chip as shown

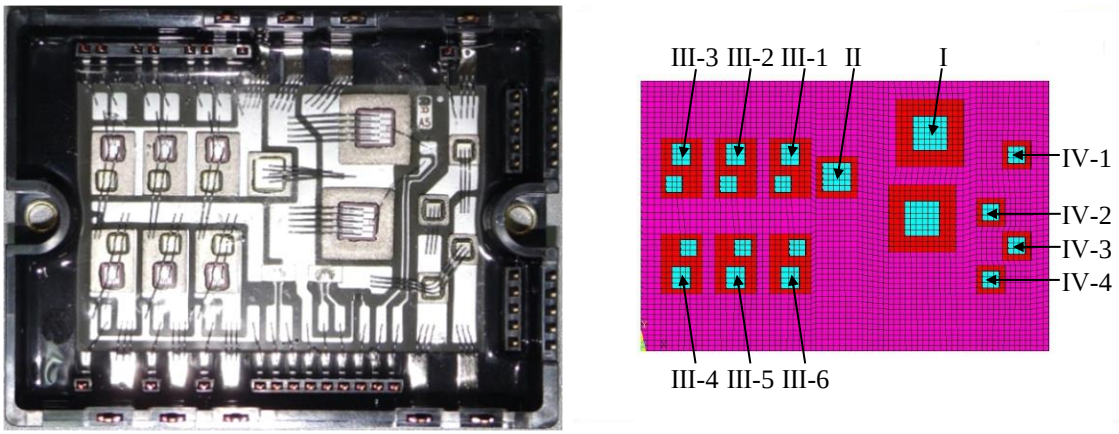

Figure 7: Photograph and full model of a power module

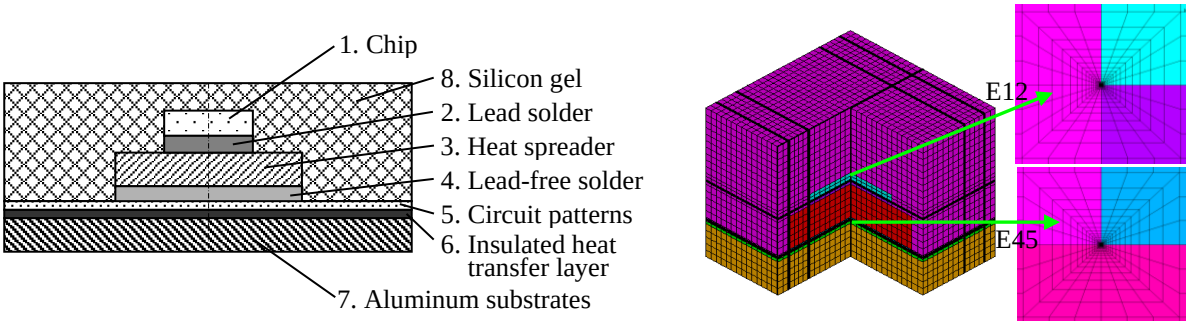

Schematic diagram of a chip structure Zooming partial model

Figure 8: Structural schematic of a chip in power module and its zooming partial model

Table 1: Material properties used in FEM analyses

No.	Elastic modulus (GPa)	Poisson ratio	Thermal expansion coefficient $\times 10^{-6}$ /K	Thermal conductivity W/m*K	Density Kg/m^3	Specific Heat J/(kg*K)
1	187.0	0.25	5.05	150.0	2330.0	678.262
2	16.1	0.44	29.4	35.2	11160.0	129.791
3	110.0	0.35	16.5	398.0	8960.0	385.186
4	41.6	0.36	21.7	64.2	7400.0	234.461
5	110.0	0.35	16.5	398.0	8960.0	385.186
6	5.4	0.34	67.0	4.0	3100.0	962.964
7	73.0	0.33	23.6	237.0	2700.0	900.162
8	0.1	0.36	50.0	0.17	980.0	1507.25

in Fig. 10, it is clarified that cracks are first generated and propagated from the vicinity of E12 during the thermal cycle tests. The singularity parameters of the stress and strain fields near E12 under the thermal cycle test conditions are calculated and summarized in Tables 2 and 3. These singularity parameters can be used to completely describe the stress and strain fields in the vicinity of E12. Furthermore, it can also be read from Table 2 that the normal stress at E12 periodically changes from compression to tension in thermal cycle tests.

4 TEMPERATURE CYCLE TESTS

In this section, we describe the results of thermal fatigue life of power modules under the thermal cycle test conditions shown in Fig.5. In the thermal cycle tests, the power modules are alternately held in -40°C and 80.0°C environments for 1800 seconds, respectively. In this study, the diagrams between the changes in electrical resistance at the chip ends and the numbers of thermal cycles are plotted as shown in Fig. 11, and the numbers of thermal cycles where the changes in electrical resistance measured every 10 thermal cycles rise sharply are defined as the thermal fatigue life of the chips. Furthermore, it is also confirmed from SEM observations that cracks are generated and propagated from the vicinity of E12 except in the case of chip II.

The thermal fatigue life of each chip of the power modules under the thermal cycle test conditions obtained by the above method are described in Table 4. It is found that the thermal fatigue life of each chip expect Chip II is about 1000 cycles, even though the position and shape of each chip are different. This means that the singularity parameters of the stress and strain fields near E12 of each chip are almost the same under the thermal cycle test conditions. As for chip II, it seems that cracks occur near E12 from the analysis results, but it is confirmed that

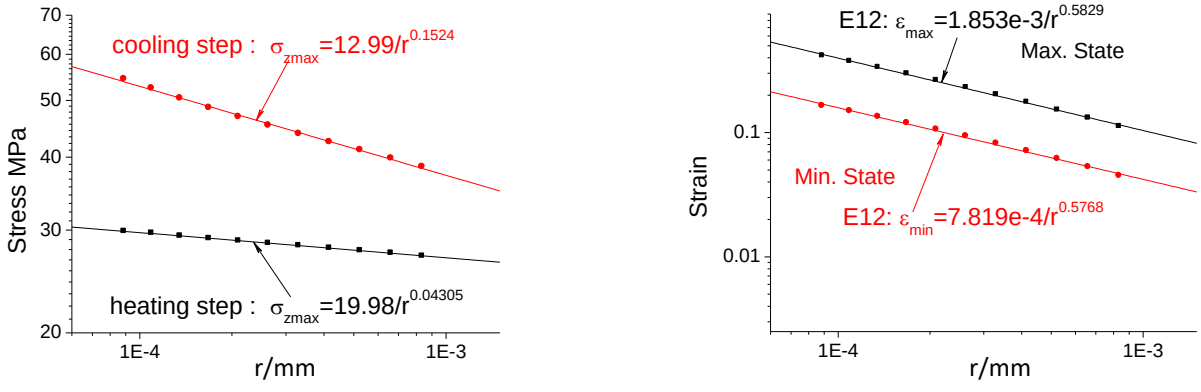

Figure 9: Maximum stress and strain distribution near E12

cracks occur near E45 from SEM observations. It is presumed that the cause of the difference between calculation and observation is a possibility of initial defects near E45.

5 EVALUATION OF THERMAL FATIGUE LIFE OF SOLDER JOINTS

In this study, the thermal cycle tests of the power modules are conducted at -40.0°C to 80.0°C. The singularity orders and singularity strength coefficients near the interface edges of the solder joints under the thermal test conditions of -40.0°C and 80.0°C are different. In the thermal cycle tests, the normal stresses at the interface edges of the solder joints periodically change from compressed state to tensile state, which is considered to be a factor causing cracks.

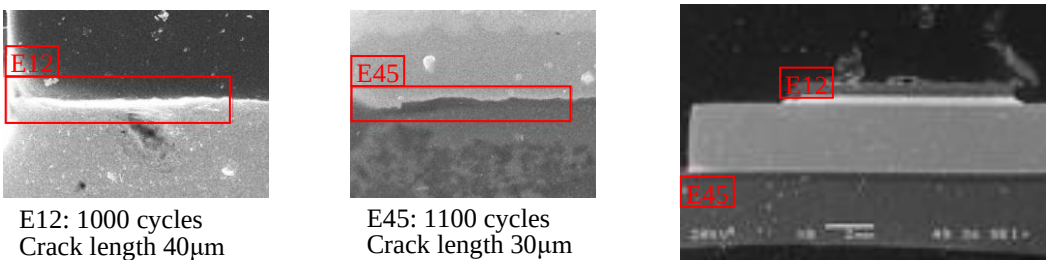

E12: 1000 cycles
Crack length 40μm

E45: 1100 cycles
Crack length 30μm

Figure 10: SEM photograph of the chip I in a power module

Table 2: Singularity parameters of stress field for E12 under thermal cycles

Chip No.	Maximum stress state in the heating step				Minimum stress state in the cooling step			
	Normal stress (MPa)		Shear stress (MPa)		Normal stress (MPa)		Shear stress (MPa)	
	δ	K_1 MPa·mm$^{\delta}$	δ	K_2 MPa·mm$^{\delta}$	δ	K_1 MPa·mm$^{\delta}$	δ	K_2 MPa·mm$^{\delta}$
II	0.04305	-19.98	0.04005	-9.202	0.1524	12.99	0.04350	13.59
III-1	0.05510	-17.90	0.03833	-9.259	0.1530	13.75	0.04383	13.76
III-2	0.05363	-18.12	0.03861	-9.241	0.1627	12.55	0.04298	13.75
III-3	0.05223	-18.32	0.03885	-9.224	0.1578	13.23	0.04306	13.65
III-4	0.05653	-17.69	0.03810	-9.272	0.1514	13.73	0.04403	13.69
III-5	0.05356	-18.12	0.03862	-9.237	0.1629	12.47	0.04297	13.75
III-6	0.05505	-17.90	0.03835	-9.254	0.1659	12.21	0.04246	13.61
IV-1	0.04098	-19.64	0.04127	-8.959	0.1588	12.54	0.04384	13.54
IV-2	0.04429	-19.21	0.04122	-8.961	0.1582	12.47	0.04392	13.49
IV-3	0.04467	-19.12	0.04097	-8.974	0.1585	12.45	0.04388	13.50

Table 3. Singularity parameters of strain field for E12 under thermal cycles

Chip No.	Maximum state		Minimum state	
	ζ	K_ε, mm$^{\zeta}$	ζ	K_ε, mm$^{\zeta}$
II	0.5829	1.853e-3	0.5768	7.819e-4
III-1	0.5701	1.700e-3	0.5563	7.650e-4
III-2	0.5745	1.661e-3	0.5588	7.514e-4
III-3	0.5751	1.659e-3	0.5606	7.446e-4
III-4	0.5684	1.717e-3	0.5543	7.734e-4
III-5	0.5734	1.670e-3	0.5586	7.531e-4
III-6	0.5731	1.685e-3	0.5560	7.700e-4
IV-1	0.5864	1.324e-3	0.5851	5.769e-4
IV-2	0.5897	1.290e-3	0.5839	5.736e-4
IV-3	0.5863	1.331e-3	0.5811	5.884e-4

5.1 Fatigue laws

It is well known that the stress or strain amplitude plays an important role in fatigue fracture problems [7-9]. In the singular stress or strain fields near the interface edge, the maximum stress or strain amplitude can be expressed by the following equations, where i represents the normal stress, shear stress and r represents the distance from the singular point.

$$\Delta\sigma_i = \frac{K_{imax}}{r^{\delta_{imax}}} - \frac{K_{imin}}{r^{\delta_{imin}}}, \quad \Delta\varepsilon = \frac{K_{\varepsilon max}}{r^{\varsigma_{max}}} - \frac{K_{\varepsilon min}}{r^{\varsigma_{min}}} \tag{4}$$

The following singularity parameters shown in Eq. (5) are required to obtain the maximum stress or strain amplitude of Eq. (4).

$$K_{\sigma max},\ \delta_{\sigma max},\ K_{\sigma min},\ \delta_{\sigma min},\ K_{\tau max},\ \delta_{\tau max},\ K_{\tau min},\ \delta_{\tau min},\ K_{\varepsilon max},\ \varsigma_{max},\ K_{\varepsilon min},\ \varsigma_{min} \tag{5}$$

Since these parameters are numerous, it is difficult and inconvenient to use them directly to construct a fatigue law. Therefore, in this study, the above parameters can be summarized into the following three typical parameters based on the theoretical consideration of average stress amplitude per unit length near the singular point at the interface edge, namely,

$$\Delta K_\sigma = \frac{K_{\sigma max}}{1-\delta_{\sigma max}} - \frac{K_{\sigma min}}{1-\delta_{\sigma min}},\ \Delta K_\tau = \frac{K_{\tau max}}{1-\delta_{\tau max}} - \frac{K_{\tau min}}{1-\delta_{\tau min}},\ \Delta K_\varepsilon = \frac{K_{\varepsilon max}}{1-\varsigma_{max}} - \frac{K_{\varepsilon min}}{1-\varsigma_{min}} \tag{6}$$

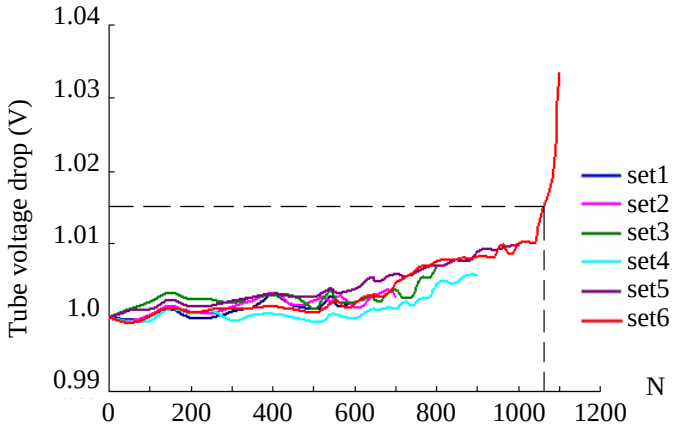

Figure 11: Voltage drop at the end of chip IV and number of thermal cycles

Table 4: Fatigue life of each chip in power module under thermal cycles

Chip No.	Thermal fatigue cycles	Crack observed cycles	Note
I	Not measured	1000	E12: 40mμ
II	830	900	E45:50 mμ
III-1	1020		
III-2	980		
III-3	1020	900	E12: 65mμ
III-4	1070		
III-5	1050		
III-6	1070		
IV-1	1070	1000	E12: 50mμ
IV-2	1060		
IV-3	1040		

where, $\Delta K_\sigma, \Delta K_\tau$ represent the effect of the multiaxial stress state, and ΔK_ε represents the effect of the strain cycle. It is empirically known that fatigue fracture mainly depends on surface force (traction) amplitude near the interface edge. Moreover, in general, the surface force amplitude near the interface edge includes the effect of the multiaxial stress state. Therefore, considering these factors comprehensively, the following four types of fatigue laws can be considered for predicting fatigue life near the interface edge.

(a) Strain controlled fatigue law

$$(\Delta K_\varepsilon)^{m_1} N_f = C_\varepsilon \tag{7a}$$

(b) Stress controlled fatigue law

$$[(\Delta K_\sigma)^2 + (\Delta K_\tau)^2]^{m_2} N_f = C_\sigma \tag{7b}$$

(c) Accelerating fatigue law

$$(\Delta K_\varepsilon)^{m_1} [(\Delta K_\sigma)^2 + (\Delta K_\tau)^2]^{m_2} N_f = C_{\varepsilon\sigma} \tag{7c}$$

(d) Accumulating fatigue law

$$[(\Delta K_\varepsilon)^{m_1} + c[(\Delta K_\sigma)^2 + (\Delta K_\tau)^2]^{m_2}] N_f = C_{\varepsilon+\sigma} \tag{7d}$$

The coefficients and constants in the fatigue laws are identified by test results, such as thermal or power cycle test results. Based on the fracture theory, the constants on the right side of the fatigue laws depend on the period ratio of the fatigue tests, and differ between the thermal cycle tests and the power cycle tests, but the exponential coefficients on the left side are the material constants and do not depend on the types of fatigue tests. Which fatigue law is most suitable for evaluating the fatigue life near interface edges of solder joints depends on the characteristics of the interface strength or the accuracy of conformity to the fatigue test results.

5.2 Fatigue laws of power module

Substituting the singularity parameters in Tables 2, 3 and the fatigue life results in Table 4 into the fatigue laws in Eq. (7) for fitting, the fatigue life evaluation equations for the power module under the thermal cycle test conditions are described in Eq. (8) as follows.

Table 5 shows the fatigue life of each chip under the thermal cycle test conditions calculated with Eq. (8). It is found that good agreement is found between the prediction results and the test results for the chips except chip II. The calculation accuracy of chip II is low because, as described above, the crack starts from the vicinity of E45 instead of E12 in the case of chip II.

(a) Strain controlled fatigue law

$$(\Delta K_\varepsilon)^{0.40} N_f = 87.90 \tag{8a}$$

(b) Stress controlled fatigue law

$$[(\Delta K_\sigma)^2 + (\Delta K_\tau)^2]^{1.74} N_f = 4.66 \times 10^8 \tag{8b}$$

(c) Accelerating fatigue law

$$(\Delta K_\varepsilon)^{0.40} [(\Delta K_\sigma)^2 + (\Delta K_\tau)^2]^{1.74} N_f = 3.93 \times 10^7 \tag{8c}$$

(d) Accumulating fatigue law

$$[(\Delta K_\varepsilon)^{0.40} + 1.89 \times 10^{-7} [(\Delta K_\sigma)^2 + (\Delta K_\tau)^2]^{1.74}] N_f = 176.10 \tag{8d}$$

In addition, the accuracy of the fatigue life evaluation equations can be improved by increasing test results and reducing dependence of the coefficients on the singularity parameters. At this stage, it is difficult to determine which equation is the best since the number of test results is limited. Considering the characteristics of creep fatigue rupture, it is speculated that the equation (8a) based on the strain-controlled fatigue law, and the equation (8d) based on the cumulative fatigue law would be more appropriate.

The fatigue life evaluation equation (8) based on the thermal cycle test results can also be used to evaluate the fatigue life of the power cycle tests. However, as described above, the exponential coefficients on the left side of the equation are material constants and do not change, but the constants on the right side of the equation change because the stress cycle ratios in the power cycle tests and the thermal cycle tests are different. The fatigue life evaluation equations based on the singularity parameters corresponding to the power cycle test conditions and test results are described in Eq. (9). The fatigue life of each chip in the power cycle tests predicted with Eq. (9) is shown in Table 6.

It is found that Eq. (9) can well express the test results of the power modules under the power cycle test conditions. As in the case of the thermal cycle tests described above, it can be read that the equation (9a) based on the strain-controlled fatigue law and the equation (9d) based on the cumulative fatigue law can well express the test results in the power cycle tests.

On the other hand, the calculations of stress and strain singularity parameters near the solder joint interface edges are complicated, and in order to directly use the fatigue laws proposed in this study, it is necessary to create a database that can easily calculate the stress and strain singularity parameters. In addition, it can be expected that the fatigue laws will be evolved, and the calculation accuracy will be improved by accumulating test results, especially the test results under different repeated loading conditions and utilizing techniques such as neuro-network.

Table 5: Fatigue life evaluations of power modules under thermal cycle tests

Chip No.	Test	Eq. (8a)		Eq. (8b)		Eq. (8c)		Eq. (8d)	
		Calc.	Error %	Calc.	Error %	Calc.	Error %	Calc.	Error %
II	830	951	14.6	934	13.1	857	3.2	946	13.9
III-1	1020	1010	-0.9	996	-2.4	966	-5.3	1004	-1.6
III-2	980	1016	3.7	1071	9.3	1044	6.5	1044	6.5
III-3	1020	1014	-0.5	1013	-0.7	986	-3.4	1014	-0.6
III-4	1070	1008	-5.7	1015	-5.1	983	-8.2	1013	-5.4
III-5	1050	1015	-3.4	1078	2.7	1049	-0.1	1046	-0.4
III-6	1070	1014	-5.2	1120	4.7	1090	1.8	1065	-0.5
IV-1	1070	1099	2.7	1005	-6.1	1060	-1.0	1050	-1.8
IV-2	1060	1110	4.7	1041	-1.8	1108	4.5	1075	1.4
IV-3	1040	1098	5.6	1047	0.7	1103	6.1	1073	3.1

Table 6: Fatigue life evaluations of power modules under power cycle tests

Chip No.	Test※	Eq. (9a)		Eq. (9b)		Eq. (9c)		Eq. (9d)	
		Calc.	Error %	Calc.	Error %	Calc.	Error %	Calc.	Error %
I	7982	7478	6.3	8695	8.9	6971	12.7	7884	6.2
II	8340	8576	2.8	9148	9.7	8411	0.8	8578	2.9
III	9529	9426	1.1	9849	3.3	9948	4.4	9427	1.1
IV	11629	12226	5.5	9679	16.8	12729	9.5	2241	5.3

※Statistical values of test results. The chips in power modules are turned off for 150s and then on for 30s again.

(a) Strain controlled fatigue law

$$(\Delta K_\varepsilon)^{0.40} N_f = 527.0 \tag{9a}$$

(b) Stress controlled fatigue law

$$[(\Delta K_\sigma)^2 + (\Delta K_\tau)^2]^{1.74} N_f = 2.0 \times 10^7 \tag{9b}$$

(c) Accelerating fatigue law

$$(\Delta K_\varepsilon)^{0.40} [(\Delta K_\sigma)^2 + (\Delta K_\tau)^2]^{1.74} N_f = 1.13 \times 10^6 \tag{9c}$$

(d) Accumulating fatigue law

$$[(\Delta K_\varepsilon)^{0.40} + 1.89 \times 10^{-7} [(\Delta K_\sigma)^2 + (\Delta K_\tau)^2]^{1.74}] N_f = 530.70 \tag{9d}$$

12 CONCLUSIONS

- In this study, we proposed zooming method for highly accurate calculation of stress and strain singularity parameters, and constructed fatigue laws using these singularity parameters. The fatigue laws can almost express the test results of fatigue life of solder joints. It is clarified that the proposed method for analyzing singularity parameters of stress and strain fields and the constructed fatigue laws are valid and useful.
- The same fatigue laws can be applied to evaluate the thermal fatigue life of solder joints with similar shapes and materials.

ACKNOWLEDGEMENT

The author would like to appreciate Prof. Xu, J. Q. of Shanghai Jiao Tong University, China for his valuable discussions and advices on this study.

REFERENCES

[1] Guo, Z. and Gonrad, H. Fatigue crack growth rate in 63Sn37Pb solder joints. *Trans. ASME, J. Electron. Packag.* (1993) **115**:159-164.
[2] Mukai, M., Kawakami, T., Hiruta, Y., Takahashi, K., Kishimoto, K. and Shibuya, T. Fatigue life estimation for solder joints in SMT-PGA packages. *Trans. ASME, J. Electron. Packag.* (1998) **120**:207-212.
[3] Takahashi, H., Kawakami, T., Mukai, M. and Ohno, N. Thermal fatigue life simulation for Sn-Ag-Cu lead-free solder joints. *J. Japan Inst. Electron. Packag.* (2004) **7**:308-313.
[4] Terasaki, T., Tanie, H., Chiwata, N., Wakano, M. and Fujiyoshi, M. Use of modified accumulated damage model to predict fatigue failure lives of Sn-Ag-Cu-based solder joints in ball-grid-array-type packages. *Trans. Japan Inst. Electron. Packag.* (2012) **5**:1-11.
[5] Liu, J., Meng, X. and Xu, J. Creep constitutive relationship and cyclic behaviors of Sn96.5Ag3Cu0.5 under high temperatures, *Int. J. Mod. Phys. B* (2008) **22**:5438-5444.
[6] ANSYS Mechanical APDL 18.0 (2017).
[7] Coffin, L. F. and Wesley R. P. A study of effects of cyclic thermal stresses on ductile metals. *Trans. ASME* (1954) **76**:931-950.
[8] Manson, S. S. *Thermal stress and low-cycle fatigue*. McGraw-Hill Book Company (1966).
[9] Kariya, Y. and Suga, T. Low-cycle fatigue properties of eutectic solders at high temperature. *Fatigue Frac. Eng. Mater.* (2007) **30**:413-419.